

First upper limits from LIGO on gravitational wave bursts

Alan J Weinstein (for the LIGO Scientific Collaboration¹)

LIGO Laboratory, California Institute of Technology, M/S 256-48, Pasadena, CA 91125, USA

E-mail: ajw@ligo.caltech.edu

Received 2 September 2003

Published 9 February 2004

Online at stacks.iop.org/CQG/21/S677 (DOI: 10.1088/0264-9381/21/5/043)

Abstract

We report on a search for gravitational wave bursts using data from the first science run of the LIGO detectors. We focus on bursts with durations ranging from 4 ms to 100 ms, and with significant power in the LIGO sensitivity band of 150 to 3000 Hz. We bound the rate for such detected bursts at less than 1.6 events per day at 90% confidence level. This result is interpreted in terms of the detection efficiency for ad hoc wave forms (Gaussians and sine-Gaussians) as a function of their root-sum-square strain h_{rss} ; typical sensitivities lie in the range $h_{\text{rss}} \sim 10^{-19}$ – 10^{-17} strain/ $\sqrt{\text{Hz}}$, depending on wave form. We discuss improvements in the search method that will be applied to future science data from LIGO and other gravitational wave detectors.

PACS numbers: 04.80.Nn, 07.05.Kf, 95.30.Sf, 95.85.Sz

1. Introduction

The LIGO Laboratory conducted its first science run (S1) during two weeks in August–September 2002 [1, 2], collecting data from three detectors (Hanford 4K or H1, Hanford 2K or H2 and Livingston 4K or L1). All three detectors were at their design configuration but not yet at design sensitivity. They were operating sufficiently stably to warrant a first science run, and with sufficiently high data quality to exercise the first generation of data analysis procedures. The LIGO Scientific Collaboration (LSC) pursued and are now presenting results of searches for four different types of gravitational wave (GW) signals: chirps from inspirals of neutron star binaries [3, 4], stochastic broadband signals from the big bang [5, 6], periodic signals from a millisecond pulsar [7, 8], and GW bursts from galactic supernovas [9], mergers

¹ The members of the LIGO Scientific Collaboration are listed in the paper by Allen and Woan for the LIGO Scientific Collaboration, in these proceedings: stacks.iop.org/CQG/21/S671.

of binary stellar-mass systems, or gamma ray burst engines [10]. Here we present the GW burst search methodology for the S1 run.

In the inspiral, stochastic and pulsar analyses, a well-defined astrophysical model was assumed, and well-tested statistical algorithms (matched filtering) were employed in the search. The wave forms of gravitational waves from burst sources such as supernovas are poorly known, so it is not clear how to employ matched filtering. We employ data analysis algorithms which can, in principle, identify bursts with a broad range of possible wave forms. We are guided by simulations of GW production in supernova core collapse (requiring axisymmetry) reported in [11, 12]. Although the wave forms resulting from these simulations are inappropriate for matched filtering, they predict that the GW bursts have short duration (between a few ms and 200 ms), possess significant energy in the LIGO frequency band (roughly 150 to 3000 Hz) and have sufficiently high strain amplitude to be observed over the S1 detector noise only if the source is very close by (a few tens of parsecs, at best).

The first detection of gravitational wave bursts requires stable, well-understood detectors, well-tested and robust data processing procedures and clearly defined criteria for establishing confidence that any signal is not of terrestrial origin. None of these elements were firmly in place as we began this first LIGO science run; rather, this run provided the opportunity for us to better understand our detectors, exercise and hone our data processing procedures and build confidence in our ability to establish detection of gravitational wave bursts in future science runs. Further, as discussed above, the sensitivities of the three LIGO detectors during S1 were such that we do not expect to detect bursts from galactic supernovas. Therefore, the goal for this analysis is to produce an upper limit on the rate for gravitational wave bursts, *even* if a purely statistical procedure suggests the presence of a signal above background.

In order to interpret our rate upper limit, we evaluate the efficiency of our search algorithms for the detection of simulated bursts injected into the data streams, using simple, well-defined wave forms (as opposed to the more complex wave forms reported in [11, 12]). We choose short duration (1 ms and 2.5 ms) broad-band Gaussians and a coarse ‘swept-sine’ set of narrow-band sine-Gaussians with ~ 9 oscillations. For such wave forms, we obtain curves of triple-coincidence detection efficiency as a function of gravitational wave form peak amplitude at the earth, averaged over source direction and incident wave (linear) polarization. We then combine our gravitational wave burst rate limits with these efficiency curves, yielding rate versus strength regions that are excluded at the 90% confidence level or higher, for the wave forms that we have examined.

2. Data processing pipeline

The search for bursts of unknown wave form in the LIGO data stream requires high data quality: stationary and Gaussian noise, low instrumental burstiness and stable detector (calibrated) response to GW signals. To ensure high quality data, we required that the band-limited RMS noise in four frequency bands the GW data channel were not significantly larger than their typical values during the run (the ‘BLRMS cut’), and that calibration lines applied to the end test masses to monitor the detector’s calibrated response to GW signals were present (the ‘calibration cut’). We also reserved approximately 10% of the triple-coincidence data as a ‘playground’ to tune our analysis pipeline.

These data quality requirements resulted in a significant reduction in the available observation time. The full S1 run comprised 408 h. All three LIGO detectors were in coincident science mode (in ‘lock’ and recording stable data) for 96.0 h. After setting aside the playground data, 86.7 h remained. The BLRMS cut retained 54.6 h, and the calibration

cut yielded a total of 35.5 h. This is the final data sample used to search for gravitational wave bursts detected in triple coincidence.

The entire analysis procedure, parameter tuning, event property estimation and all other optimizations were developed using the playground data, and frozen before applying the analysis to the full S1 dataset. It then became clear that many of the procedures and tunings were less than optimal, for a variety of reasons. We have chosen to present the results of this first analysis in this paper, with no claim of optimal performance, and to apply improved methods and optimizations to the analysis of S2 and future datasets.

After the data quality cuts described above, the GW data channel from each of the three detectors was processed through parallel single-detector analysis pipelines, producing single-detector event triggers. In a second step, temporal coincidences of event triggers from all three detectors are found and tested for consistency. The resulting list of triple-coincident event triggers constitutes our sample of candidate GW burst events.

The single-detector analysis pipeline proceeds as follows. The GW data channel (uncorrected for the detector response to GWs) are read in to the LIGO data analysis system (LDAS) where it is prefiltered: the data are high-pass filtered with corner frequency of 150 Hz, and then approximately whitened above 150 Hz. After prefiltering, the data are passed to *event trigger generators* which identify data stretches in which a GW burst may be present. We use two different techniques to identify event triggers from the prefiltered gravitational wave data channel at each detector. One technique, which we refer to as SLOPE, is based on [13, 14]. The second technique, which we refer to as TFCLUSTERS, is described in [15]. These two algorithms identify bursts in noisy data using very different approaches, and may be expected to perform differently for different wave form morphologies. These algorithms are implemented within the LIGO data analysis environment [16].

The SLOPE algorithm identifies candidate gravitational wave bursts by thresholding on the output of a linear filter applied to the prefiltered gravitational wave data in the time domain. We choose a filter that is essentially a differentiator (in time), and trigger on a slope in the data stream which is (statistically) inconsistent with expectations from white Gaussian noise. The SLOPE algorithm is most sensitive when the detector noise in the strain channel is whitened. The parameters of the SLOPE filter have been tuned so that its highest sensitivity is for bursts in which the signal amplitude is increasing linearly with time for ten data samples ($10 \times 61 \mu\text{s}$), resulting in best sensitivity for burst signals oscillating at 1.1 kHz. A peak search algorithm is then applied to the filter output to search for maxima indicating the presence of bursts. Peaks greater than some preset threshold result in an event trigger. For this analysis, the threshold was fixed and did not adapt to changing noise levels.

The TFCLUSTERS event trigger generator is a detection algorithm which identifies connected regions (*clusters*) in a time-frequency plane where the power is not consistent with the expectations for stationary, coloured Gaussian noise. The prefiltered data are used to construct a time-frequency spectrogram from 2880 periodograms calculated from 125 ms long non-overlapping subsegments of the 6 min long segment. A first level of thresholding is applied to the spectrogram, resulting in a high-contrast pixelization. All the pixels of the spectrogram with power larger than some threshold are labelled as *black pixels*, while pixels below the threshold are labelled as white pixels. In the absence of signals, any pixel in the spectrogram has, to a good approximation, an equal and independent probability p of being black, in each frequency band. Because of this procedure, the effective threshold for black pixels varies in response to changing detector noise levels; the threshold is ‘adaptive’, as opposed to the fixed threshold employed in the SLOPE algorithm. The black pixels are then clustered, to look for bursts of excess power in a limited region of the time-frequency plane. All clusters containing at least five pixels constitute an event trigger.

For each event trigger produced by the SLOPE or TFCLUSTERS event trigger generator, an entry is made in a trigger database, containing an estimate of the event start time and duration and (algorithm-dependent) estimates of the frequency band, energy in the burst event and signal-to-noise ratio for the burst event.

Single-detector burst event triggers generated by the two algorithms discussed above were dominated by fluctuations in the detectors' noise (fake bursts), not GW signals. These triggers were used to search for temporal coincidence between the three LIGO detectors. We rely heavily on triple coincidence to minimize the resulting fake rate. For this analysis, the coincidence window for TFCLUSTERS and SLOPE triggers were conservatively set at ± 500 ms and ± 50 ms, respectively. The TFCLUSTERS algorithm also provided an estimate of the frequency band of the burst event candidate in each detector; we required (loose) consistency between the three such estimates in a triple-coincidence candidate.

3. Background and excess coincidence rate

The analysis pipeline described in the previous section was applied to the data from the three LIGO detectors, separately for the TFCLUSTERS and SLOPE algorithms. A handful of triple-coincidence burst event candidates survived the pipeline from each algorithm (but with no event shared by both algorithms). To establish whether these events are consistent with expectations from detector noise and accidental coincidence, the background rate was determined.

The accidental coincidence rate can be estimated by time-delayed coincidences between event triggers from the Hanford detectors (H1 and H2) and from the Livingston detector (L1). In order to avoid correlations between successive triggers from a single detector, and to ensure approximate stationarity of the burst event trigger rate, we restricted the time shifts to 100 s or less, in 8 s steps (for a total of 24 time-shifted coincidence measurements). The resulting distributions of numbers of background events are consistent with the expectation from the Poisson statistics. From these distributions, we estimate the number of background events to be 10.1 ± 0.6 for the TFCLUSTERS algorithm and 1.7 ± 0.3 for the SLOPE algorithm, over the 35.5 h observation time.

The SLOPE analysis pipeline employed a fixed threshold for identifying burst triggers. The detectors' noise levels varied by an order of magnitude or more during S1, sometimes over time scales of minutes. The resulting rate of (noise-induced) burst event triggers from the SLOPE algorithm varied correspondingly, resulting in considerable non-stationarity in the single-detector and triple-coincident burst rate. These variations make the estimation of background rate problematical. For this reason, we choose to quote rate results from the TFCLUSTERS analysis pipeline only, where adaptive thresholding was used. The SLOPE algorithm was, however, competitive with the TFCLUSTERS algorithm in its efficiency for detecting gravitational wave signals, as discussed below. Future results will make use of adaptive thresholding in the SLOPE analysis pipeline.

An excess in the number of coincident (zero-time shift) events over the estimated background can be estimated statistically. Here we make use of the unified approach of Feldman and Cousins [17], defining confidence bands at various confidence levels on the number of excess events using only the TFCLUSTERS event trigger generator algorithm. The upper bounds of the confidence bands are taken to be the upper limit on the number of signal events, at that confidence level. At the 90% confidence level, the TFCLUSTERS search yielded an upper limit of 1.6 events per day.

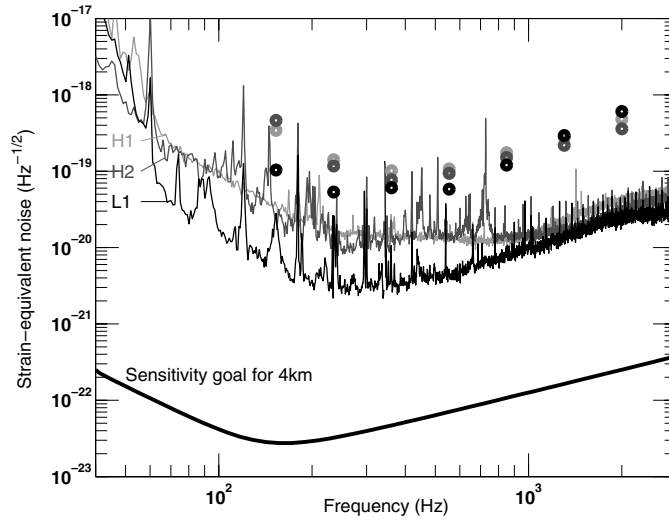


Figure 1. Typical sensitivities of the three LIGO interferometers during the S1 data run, in terms of equivalent strain noise amplitude density, are shown as lines with progressively lighter shadings for the L1, H2 and H1 detectors. The points are the root-sum-square strain (h_{rss}) of sine-Gaussian bursts for which our analysis pipeline is 50% efficient for burst signals incident on a single detector with optimal source direction and polarization; the three shadings correspond to the three different detectors.

4. Burst simulations, efficiencies

A burst event rate measurement or upper limit can only be interpreted in the context of some assumed source. Here, we assume that the GW burst signal has a specific wave form, and we evaluate the efficiency for the detection of such a wave form by the three LIGO interferometers as a function of the burst amplitude. As mentioned in section 1, we consider two classes of wave forms: narrow-band sine-Gaussians with central frequencies ranging from 100 Hz to 2000 Hz and containing roughly nine cycles in a Gaussian envelope; and broad-band Gaussians of the form $h(t) = h_0 \exp(-t^2/\tau^2)$, with τ of 1 ms or 2.5 ms. We quantify the amplitude of these bursts with the root-sum-square (rss) amplitude spectral density, in units of dimensionless strain per root Hz: $h_{\text{rss}} \equiv \sqrt{\int |h|^2 dt}$.

To evaluate the detection efficiency for such bursts incident on a single detector with optimal source direction and polarization, we generate a digitized burst wave form $h(t)$ with a specific wave form and value of h_{rss} , filter it through the calibration function to convert it from strain to GW data channel counts, add it to the raw GW data channel, pass the resultant data through the standard analysis pipeline described in section 2, and see if it is detected as an event trigger. We repeat this many times, using data samples throughout the S1 run in order to incorporate any time dependence to the detection efficiency. We thus obtain an average of the detection efficiency as a function of burst event amplitude for that wave form, detector and event trigger generator algorithm. The amplitudes at which the efficiencies are 50% for the narrow-band sine-Gaussians roughly track the detectors' noise equivalent strain sensitivity, as shown in figure 1.

We evaluate the efficiency for triple coincidence detection, averaged over source direction and polarization, via a simple Monte Carlo integration. The results of this procedure are curves of triple-coincidence efficiency versus GW burst amplitude h_{rss} for each wave form,

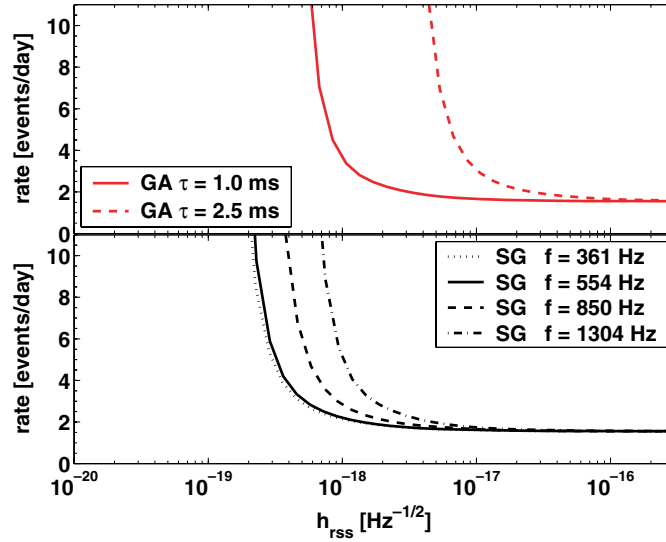


Figure 2. Rate versus h_{rss} for detection of specific wave forms using the TFCLUSTERS analysis pipeline. The region above and to the right of the curves is excluded at 90% confidence level or greater. The effect of the 20% uncertainty in the detector response is included. Top: for Gaussians with $\tau = 1.0$ ms and $\tau = 2.5$ ms. Bottom: for sine-Gaussians with $Q = 9$ and central frequency $f_0 = 361, 554, 850$ and 1304 Hz.

Table 1. Sensitivity in terms of h_{rss} (units of $\text{Hz}^{-1/2}$) at 50% efficiency to various wave forms in the S1 run from TFCLUSTERS and SLOPE.

	TFCLUSTERS	SLOPE
Gaussian $\tau = 1.0$ ms	1.0×10^{-18}	2.6×10^{-18}
Gaussian $\tau = 2.5$ ms	8.2×10^{-18}	3.6×10^{-17}
Sine-Gaussian $f_0 = 153$ Hz	1.6×10^{-18}	1.2×10^{-17}
Sine-Gaussian $f_0 = 254$ Hz	5.1×10^{-19}	2.8×10^{-18}
Sine-Gaussian $f_0 = 361$ Hz	3.8×10^{-19}	1.1×10^{-18}
Sine-Gaussian $f_0 = 554$ Hz	4.2×10^{-19}	5.6×10^{-19}
Sine-Gaussian $f_0 = 850$ Hz	7.3×10^{-19}	6.1×10^{-19}
Sine-Gaussian $f_0 = 1304$ Hz	1.4×10^{-18}	6.7×10^{-19}
Sine-Gaussian $f_0 = 2000$ Hz	2.3×10^{-18}	2.5×10^{-18}

averaged over source direction and polarization and over the S1 run. The GW burst amplitude h_{rss} for each wave form at which our detection efficiency is 50% is given in table 1. The largest source of systematic error associated with this detection efficiency evaluation is due to imperfect understanding of the calibrated detector response. We conservatively assign a 20% error to our estimate of the response of the detector to a burst event with a given amplitude h_{rss} .

5. Results: rate versus strength

The burst event rate upper limits obtained above, divided by the curves of efficiency versus burst amplitude described above, result in the curves shown in figure 2. These curves represent the

upper limits that we set for different wave forms, using the TFCLUSTERS analysis pipeline, as expressed in the plane of event rate versus h_{rss} . The region of rate versus amplitude to the right and above the curve is excluded at 90% confidence level or higher.

A careful study of the response of our pipeline to wave forms motivated by astrophysical models, such as the stellar core collapse simulations described in [11], is in progress. However, to set the scale, it can be noted that the louder wave forms reported in [11], from a supernova at 100 pc, will produce a strain at the earth of $h_{\text{rss}} \sim 3 \times 10^{-19} \text{ Hz}^{-1/2}$.

6. Improvements for S2

LIGO's second science run (S2) accumulated data for 8 weeks in early 2003. At most frequencies, the noise in the three LIGO detectors was improved compared to the noise level of the S1 data presented here by a factor of 10. Some improvements in the stability of the noise were also achieved. The in-lock duty cycles of the detectors were comparable to those obtained during S1, but tighter monitoring of the detectors' noise levels and calibration should lead to significantly less loss of data than was suffered in S1. Even without improvements in our analysis methodology, we expect to obtain results from the S2 data that are an order of magnitude more sensitive in amplitude, and observation times that are increased by at least a factor of four over the results presented here.

Based on lessons learned during the S1 analysis, we are preparing numerous improvements and additions to our search methodology for the S2 dataset. The GW data channel prefiltering will be better optimized. The event trigger generators will be better tuned and optimized for best efficiency and fake rate. Thresholds will be chosen to yield much less than one fake (noise) event over the entire observation period. Many different burst detection algorithms will be evaluated. We will identify and employ effective and safe vetoes on auxiliary channels. In order to dramatically suppress accidental coincidences, we will determine event trigger start times to sub-millisecond precision, and require consistency between calibrated burst amplitudes, frequency bands and wave forms between the detectors. In order to reduce our dependence on the least sensitive detector in the network, we will consider double-coincident events. We will pursue more, and better motivated, simulations, (such as the supernova simulations in [11]), and establish clear methods to translate our results to arbitrary burst wave forms. Finally, and crucially, we are developing criteria by which we can establish confidence in the detection of gravitational wave bursts both statistically and as a single large amplitude burst event. For single burst event candidates, we will use information from all available detectors to reconstruct our best estimates of the gravitational wave direction, polarization and wave form.

Acknowledgments

The authors gratefully acknowledge the support of the United States National Science Foundation for the construction and operation of the LIGO Laboratory and the Particle Physics and Astronomy Research Council of the United Kingdom, the Max-Planck-Society and the State of Niedersachsen/Germany for support of the construction and operation of the GEO600 detector. The authors also gratefully acknowledge the support of the research by these agencies and by the Australian Research Council, the Natural Sciences and Engineering Research Council of Canada, the Council of Scientific and Industrial Research of India, the Department of Science and Technology of India, the Spanish Ministerio de Ciencia y Tecnologia, the

John Simon Guggenheim Foundation, the David and Lucile Packard Foundation, the Research Corporation and the Alfred P Sloan Foundation.

References

- [1] LIGO Scientific Collaboration 2003 LIGO and GEO detector configuration during S1 *Preprint gr-qc/0308043*
- [2] See talks by Weiss R, Sigg D and O'Reilly B 2003 *Proc. 5th Edoardo Amaldi Conf. on Gravitational Waves (Tirrenia, Italy, July 6-11, 2003)*
- [3] LIGO Scientific Collaboration 2003 Analysis of LIGO data for gravitational waves from binary neutron stars *Preprint gr-qc/0308069 (Phys. Rev. D at press)*
- [4] Gonzalez G 2004 *Class. Quantum Grav.* **21** S691
- [5] LIGO Scientific Collaboration 2003 Analysis of first LIGO science data for stochastic gravitational waves *Phys. Rev. D to be submitted*
- [6] Whelan J 2004 *Class. Quantum Grav.* **21** S1059
- [7] LIGO Scientific Collaboration 2004 *Phys. Rev. D* **64** (*Preprint gr-qc/0308050*)
- [8] Talks by Allen B and Woan G 2003 *Proc. 5th Edoardo Amaldi Conf. on Gravitational Waves (Tirrenia, Italy, July 6-11, 2003)*
- [9] Fryer C L, Holz D E and Hughes S A 2002 *Astrophys. J.* **565** 430
- [10] Talks by Kokkotas K and van Putten M 2003 *Proc. 5th Edoardo Amaldi Conf. on Gravitational Waves (Tirrenia, Italy, July 6-11, 2003)*
- [11] Zwerger T and Müller E 1997 *Astron. Astrophys.* **320** 209
- [12] Dimmelmeier H, Font J A and Müller E 2001 *Astrophys. J. Lett.* **560** L163
- [13] Arnaud N *et al* 1999 Detection of gravitational wave bursts by interferometric detectors *Phys. Rev. D* **59** 082002
- [14] Pradier T *et al* 2001 Efficient filter for detecting gravitational wave bursts in interferometric detectors *Phys. Rev. D* **63** 42002
- [15] Sylvestre J 2002 *Phys. Rev. D* **66** 102004
Sylvestre J 2002 *PhD Thesis* MIT
- [16] LIGO data analysis system (LDAS) version 0.4.0 2002 <http://www.ldas-cit.ligo.caltech.edu>
- [17] Feldman G J and Cousins R D 1998 *Phys. Rev. D* **57** 3873